

Exergy Analysis of a GTL Process Based on Low-Temperature Slurry F–T Reactor Technology with a Cobalt Catalyst

Carmine L. Iandoli and Signe Kjelstrup*

Department of Chemistry, Norwegian University of Science and Technology (NTNU), Trondheim, Norway

Received December 19, 2006. Revised Manuscript Received March 30, 2007

Interest in the gas-to-liquid process (GTL) using Fischer–Tropsch reactors (F–T) has increased in recent years because of its potential to replace ordinary petroleum with sulfur-free fuels. However, the efficiency of the process is still low compared with current routes; a large amount of the initial exergy of the gas is used to convert it into liquid fuel. In the present study, we analyze the overall thermodynamic efficiency of a GTL process and point out the main sources of entropy production. Next, we use exergy analysis to establish the impact of catalyst selectivity and of thermal losses on the process efficiency. In particular, we report the effect of selectivity losses in the F–T reactor and reformer, and the impact of high-temperature heat integration across the reforming unit.

1. Introduction

The Fischer Tropsch (F–T) synthesis was originally developed in Germany in the 1920s by Franz Fischer and Hans Tropsch; their aim was to use a mixture of CO and H₂ (referred to as synthesis gas, syngas) to produce hydrocarbons, chemicals, and liquid fuels. The production of syngas was achieved by coal gasification, and 10 small-scale plants (production < 1 million ton/year) were built before World War II in a push for petroleum independence. After World War II, oil was available, and commercial applications of F–T synthesis were less attractive. New plants based on F–T synthesis were built after 1955 in South Africa to overcome the oil shortage caused by the embargo imposed by the Arab Emirates (in 1973) and United Nations (in 1981). The process feedstock was still coal (coal-to-liquid, CTL). In the 1990s, natural gas was discovered in South Africa offshore, and a process using gas as feedstock was implemented. The process, known as gas-to-liquid (GTL), was based on two steps: first, steam reforming of natural gas into syngas and, then, Fischer–Tropsch synthesis of syngas into synthetic liquid fuels. A first plant was built in Mossel Bay (1992). Details about the historical development of F–T technology were reported by Freerks.¹

The history of F–T synthesis shows that, although the technology has been available since the 1920s, its practical use has been pushed by a lack of crude oil (high oil prices). Recently (2004–2006), the massive growth of GNP in China and India has caused crude oil prices to rise continuously, and F–T synthesis (including both coal and biomass as feedstock, BTL) has become once more an appealing technology.

Recent interest in F–T technology especially in Europe and South America is driven by a focus on the gasification of biomass into fuel² (BTL). Moreover, European oil companies are also interested in GTL as a business opportunity outside Europe. New CTL plants are planned in China and the U.S.A.

The Shell GTL plant in Malaysia has been in operation since 1993, and a new plant owned by Qatar Petroleum and Sasol will start production in Qatar in early 2007. GTL is seen as the main alternative to liquefied natural gas for monetizing so-called stranded gas worldwide.

The GTL diesel fuel has near zero sulfur content and aromatic components and a very high cetane number. For this reason, GTL diesel fuels are able to reduce exhaust emissions from a variety of diesel engines.³ The production of synthetic fuels implies CO₂ emissions, therefore, and a well-to-wheel analysis shows that the overall CO₂ emissions are still higher than those from the conventional oil-refining route.

The overall energy balance and CO₂ emission sources are understood, but the relative impact of different technology elements of the GTL process have not been studied. How will high-temperature heat integration (HTHI) in the syngas unit affect the energy efficiency of the GTL plant, and how does it compare to improvements in the selectivity of the F–T synthesis? An exergy analysis can provide better understanding of the fundamental reason for the efficiency losses in a GTL plant.

Only one exergy analysis is known to us, based on BTL,² but a number of life cycle analyses focusing on first law efficiency have been published by the oil companies. Our aim is therefore to study what the initial exergy of the natural gas exactly is used for, and where and why exergy is lost in the process.

On the basis of process simulations of a promising GTL concept available today using Pro/II (Aspen/SimSci), the exergy balance and exergy losses of the process have been calculated. The relative impact of the following parameters has been analyzed:

- improvement in F–T catalyst selectivity
- once-through operation of the F–T reactor
- high-temperature heat integration across the autothermal reformer (ATR) (HTHI, no metal dusting)
- high-temperature heat integration: gas-heated reforming (GHR)
- and syngas production via ideal low- and high-temperature catalytic partial oxidation (LTCPO and HTCPO).

* Author to whom correspondence should be addressed. E-mail: signe.kjelstrup@chem.ntnu.no.

(1) Freerks, R. AIChE Spring National Meeting, New Orleans, LA, 2003.

(2) Prins, M. J.; Ptasiński, K. J.; Janssen, F. J. J. G. *Fuel Process. Technol.* **2005**, *86*, 375–389.

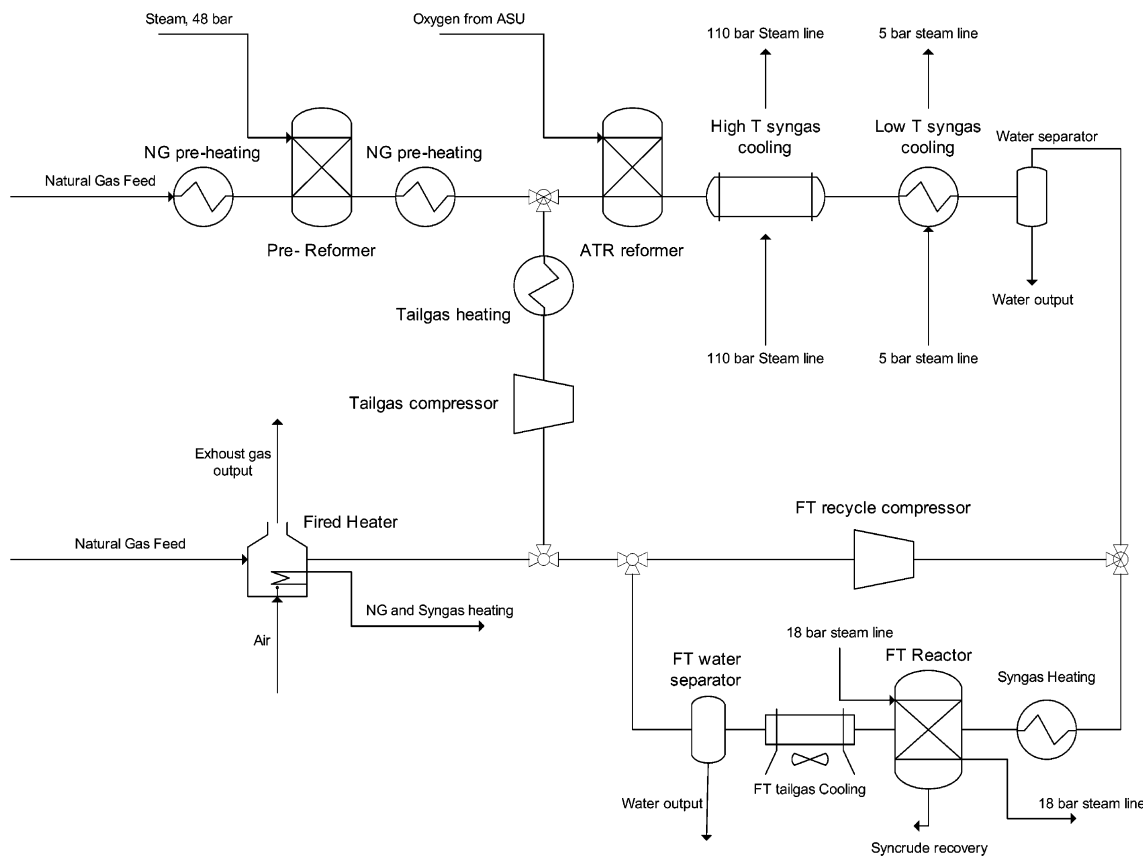


Figure 1. Schematic flowsheet (power plant and ASU not shown).

91 Ideal CPO (no CO₂ formation) has not been proved feasible
 92 in practical applications so far; the reforming unit of the
 93 reference case is thus a catalytic ATR.¹⁰ ATR is the preferred
 94 syngas technology today since it provides a better H₂/CO ratio
 95 compared to all alternatives.²⁶ However, it uses pure oxygen

(internal-fired steam reforming) as feedstock; therefore, an air
 separation unit (ASU) is included.

96
 97
 98 Due to the high selectivity of Co-based catalysts, a lot of
 99 effort has been spent on developing and improving catalysts
 100 for use in industrial applications. This study is based on the
 101 low-temperature slurry-phase Fischer–Tropsch reactor technol-
 102 ogy with a cobalt catalyst. Pilot units based on this technology
 103 have been built by Sasol, Statoil, ENI, and Exxon.

2. GTL Technology and Reference Case

104
 105 A GTL plant consists of three main process units: a reforming
 106 unit where syngas is produced, a F–T unit where syngas is
 107 converted into liquids (synchrude), and a product upgrading unit
 108 where synchrude is upgraded into synthetic diesel and naphta. Our
 109 investigations do not include the product upgrading unit because it
 110 is not heat-integrated with other main process units; hence, the
 111 design will not be affected by the parameters studied here. A
 112 schematic process flowsheet is shown in Figure 1. In the following,
 113 we will describe how the GTL concept was modeled.

114
 115 **2.1. Base Case Model Boundaries.** Figure 1 shows the process
 116 steps included in the GTL model. Natural gas feed is preheated,
 117 mixed with steam and pure oxygen from the ASU, and sent into
 118 the ATR. The ATR converts natural gas, oxygen, and steam into
 119 synthesis gas at approximately 1300 K. Syngas is then cooled to
 120 separate water. Latent heat is recovered in a waste heat boiler
 121 producing both high- and low-pressure steam (110 and 5 bar).
 122 Synthesis gas is fed into the slurry-phase F–T reactor where it is
 converted into “synthetic” wax. Since the stability of the F–T

(3) Schalberg, P. W.; Myburgh, I. S.; Botha, J. J.; Roets, P. N.; Viljoen, C. L.; Dancuart, L. P.; Starr, M. E. SAE International Fall Fuels & Lubricant Meeting & Exposition, Tulsa, Oklahoma, 1997; paper 972898.
 (4) Maretto, C.; Krishna, R. *Catal. Today* **1999**, *52*, 279–289.
 (5) Yates, I. C.; Satterfield, C. N. *Energy Fuels* **1991**, *5*, 168–173.
 (6) Hall, K. R. *Catal. Today* **2005**, *106*, 243–246.
 (7) Aasberg-Petersen, K.; Bak Hansen, J. H.; Christensen, T. S.; Dybkjaer, I.; Seier Christensen, P.; Stub Nielsen, C.; Winter Madsen, S. E. L.; Rostrup Nielsen, J. R. *Appl. Catal.* **2001**, *221*, 379–387.
 (8) Storsæter, S.; Borg, Ø.; Blekkan, E. A.; Holmen, A. *J. Catal.* **2005**, *231*, 405–419.
 (9) Dancuart, L. P.; de Haan, R.; de Klerk, A. *Stud. Surf. Sci. Catal.* **2004**, *152*, 482–528.
 (10) Gunardson, H. *Industrial Gases in Petrochemical Processing*; Marcel Dekker: New York, 1997.
 (11) Cornelissen, R. L.; Hirs, G. G. *Energy Conversion and Management* **1998**, *39*, 1821–1826.
 (12) Szargut, J. *Exergy Method: Technical and Ecological Applications*; WIT Press: Southampton, England, 2005.
 (13) Ahón, V. R.; Costa, E. F.; Monteagudo, J. E. P.; Fontes, C. E.; Biscaia, E. C.; Lage, P. L. C. *Chem. Eng. Sci.* **2005**, *60*, 677–694.
 (14) Dry, M. E. *Stud. Surf. Sci. Catal.* **2004**, *152*, 533–600.
 (15) Li, J.; Zhan, X.; Zhang, Y.; Jacobs, J.; Das, T.; Davis B. H. *Appl. Catal., A* **2002**, *228*, 203–212.
 (16) Donnelly, T. J.; Yates, I. C.; Satterfield, C. N. *Energy Fuels* **1988**, *2*, 734–739.
 (17) Schulz, H.; Claeys, M. *Appl. Catal., A* **1999**, *186*, 91–107.
 (18) Grabke, H. J. *Mater. High Temp.* **2000**, *17* (4), 483.
 (19) Kotas, T. J. *The Exergy Method of Thermal Plant Analysis*; Krieger: Malabar, Florida, 1995.
 (20) *Hydrocarbon Selectivity of Cobalt Fischer-Tropsch Catalysts*; Massachusetts Institute of Technology: Cambridge, MA, 1991; DE91018065.
 (21) van Dijk, H. A. J.; Heobink, J. H. B. J.; Schouten, J. C. *Chem. Eng. Sci.* **2001**, *56*, 1211–1219.
 (22) Johannessen, E.; Kjelstrup, S. *Chem. Eng. Sci.* **2005**, *60*, 3347–3361.

(23) Nummendal, L.; Røesjorde, A.; Johannessen, E.; Kjelstrup, S. *Chem. Eng. Process.* **2005**, *44*, 429–440.
 (24) Storsæter, S.; Borg, Ø.; Holmen, A. *J. Catal.* **2005**, *231*, 405–419.
 (25) Rabe, S.; Truong, T.-B.; Vogel, F. *Appl. Catal., A* **2005**, *292*, 177–188.
 (26) Higman, C.; van der Burgt, M. *Gassification*; Elsevier: New York, 2006.

123 catalyst will be affected by the partial pressure of water, we have
 124 assumed that maximum per pass conversion in the F–T reactor is
 125 60%.⁸ As a consequence, the reactor tailgas is recycled to allow
 126 for a reasonable overall yield across the F–T unit. Moreover, part
 127 of the syngas is converted into light hydrocarbons (C₁ to C₄), which
 128 can be condensed and recovered at cryogenic conditions. A fraction
 129 of the F–T tailgas is recycled back to the ATR, and recycled CO₂
 130 adjusts the H₂/CO ratio close to the optimum.

131 To get a realistic picture of the exergy losses in a GTL plant,
 132 the steam and power system has been included in the model. The
 133 steam and power system balances the production/consumption of
 134 heat, steam, and mechanical energy in the GTL plant. Steam
 135 generated from heat recovery in the syngas and F–T unit is used
 136 to cover both steam and power demands in the GTL plant and the
 137 air separation unit. The ASU has not been modeled and simulated,
 138 but its exegeric efficiency has been included on the basis of data
 139 found in the literature.¹¹ The energetic cost for oxygen production
 140 used in our model was 0.35 MWh/tonO₂. This value is much higher
 141 than the oxygen exergy reported by Szargut¹² and reflects the low
 142 efficiency of cryogenic separation in general. The amount of oxygen
 143 needed by the ATR is derived from the process simulations.

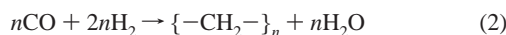
144 **2.2. Modeling the Units.** Flowsheets of the GTL process and
 145 steam system have been developed. The process layout, illustrated
 146 in Figure 1, indicates the boundaries set in the investigation; the
 147 power plant flowsheet is not shown. Since the F–T unit has a low
 148 degree of conversion of reactants, the flowsheet has a recycle loop
 149 for tailgases. The process simulation model includes the syngas
 150 and the F–T unit. The models used for the reactors in these units
 151 are described below.

152 **2.2.1. Syngas Unit.** The chemical reactions, which quantitatively
 153 best describe the ATR are



157 A detailed description of the ATR chemical kinetics can be found
 158 in the literature.¹⁰ Detailed modeling of the ATR is very complex
 159 and requires detailed chemical kinetics and extensive use of
 160 computational fluid dynamics. However, determining the overall
 161 heat and mass balances of the ATR is based on specifying that
 162 chemical equilibrium will be reached (using existing model
 163 subroutines for equilibrium reactors available with Aspen/ProII).

164 **2.2.2. Fischer–Tropsch Unit.** Rather detailed models of slurry-
 165 phase F–T reactors can be found in the literature.¹³ The F–T slurry
 166 reactor has been modeled as a continuously stirred tank reactor
 167 operating at constant temperature (similar to Prins, et. al² in their
 exergy analysis of F–T synthesis in BTL). These authors assumed
 that the essence of the F–T synthesis on a cobalt catalyst is
 described by the simple reaction



169 while the water–gas shift reaction can be neglected. The consump-
 170 tion of syngas is modeled with a kinetic equation of a Langmuir–
 Hinshelwood type:⁵

$$171 -R_{\text{CO}} + 2\text{H}_2 = \frac{ap_{\text{CO}}p_{\text{H}_2}}{(1 - bp_{\text{CO}})^2} \quad (3)$$

The parameters according to Maretto, Krishna⁴ are

$$172 a = 8853.3 \exp\left[4449.1\left(\frac{1}{493.15} - \frac{1}{T}\right)\right] \text{ mol}/(\text{s}\cdot\text{kg}_{\text{cat}}\cdot\text{bar}^2) \quad (4)$$

To model the product distribution of F–T synthesis, we chose the

$$b = 2.226 \exp\left[8236\left(\frac{1}{493.15} - \frac{1}{T}\right)\right] \text{ 1/bar} \quad (5)$$

most common approach, the so-called Anderson–Schulz–Flory
 distribution:

$$x_N = (1 - \alpha_{\text{ASF}})\alpha_{\text{ASF}}^{N-1} \quad (6)$$

This model assumes a chain-growth mechanism, defined through
 the α_{ASF} parameter. A last assumption for the F–T reactor is that
 the reactor produces only paraffins (no olefins). This assumption,
 common in similar analyses,³ is supported by the use of a cobalt
 catalyst which is known to produce mostly paraffins with limited
 amounts of olefins. In the real operation of Co-based F–T reactors,
 the production of olefins is usually low for heavier hydrocarbons,
 while up to 30% olefins has been observed in the naphta range.¹⁴
 For this investigation, we fixed both the pressure and temperature
 of the reactor, while the *per pass* conversion of H₂ was fixed to
 60%. A larger *per pass* conversion will increase the amount of
 water in the reactor, and recent studies²⁴ show that high concentra-
 tions of water deactivate the catalyst rapidly. A summary of the
 operating conditions of the F–T reactor is reported in Table 1.

Equation 3 is often reported as a suitable rate.¹⁴ It shows that
 the reaction rate increases with the partial pressure. However, there
 is no direct effect of the partial pressure of water, as in other
 models.¹⁵

More advanced models than equation 6 take into account the
 higher selectivity toward species with a higher carbon number
 observed in experiments, see for example Donnelly, et. al¹⁶ and
 Schultz.¹⁷

2.2.3. Power and Steam Production Unit. The GTL process
 consists of thermocycles. Natural gas is first preheated in a fired
 heater and then sent into the ATR from where it is released at 1300
 K. This temperature is too high for F–T synthesis, and water vapor
 needs to be removed. The syngas (eq 1) is therefore cooled in a
 waste heat boiler to 310 or 320 K depending on the availability of
 cooling water. After condensing out the water, the syngas is
 preheated to approximately 240 °C and fed to the F–T reactor. In
 these steps, a large amount of heat is made available. Another source
 of heat, but at a lower temperature, is the F–T reactor (reaction 2
 is strongly exothermic, $\Delta H = -159$ kJ/mol at 500 K and 40 bar).

Pressure levels and the sources of heat from the process are given
 in Table 2. The steam plant uses heat from syngas waste heat and
 the F–T reactor to produce saturated steam, which is later
 superheated using heat obtained by burning the F–T tailgas in the
 fired superheater. A design criterion for the superheating of steam
 is that the liquid fraction at the turbines output must not exceed
 3%. Superheated steam is expanded in turbines to produce power
 for the ASU and other users (pumps and compressors), while surplus
 power is exported. If tailgas exergy does not cover the needs of
 the superheaters, natural gas must be supplied to the fired heater.

3. Selection of Process Parameters

As a reference case is chosen a state-of-the-art GTL process based
 on low-temperature Fischer–Tropsch (LTFT) slurry-phase cobalt
 catalyst synthesis. The reactor layout is thus not a variable of our
 investigation.

Test case studies have been divided into two groups: F–T reactor
 performance (cases 1 and 2) and reforming technology (cases 3–5),
 and they are listed below:

1. F–T Catalyst Selectivity. F–T selectivity (as defined in eq
 9, see below) was increased by changing the value of α_{ASF} in eq 6.
 The catalyst selectivity was increased by 5%, relative to the
 reference case.

2. Once-Through Operation of the F–T Reactor. We assumed
 that “per pass” hydrogen conversion can be raised to 90%. Under
 this condition, there is no need for recycling F–T tailgas.

3. High-Temperature Heat Integration (HTHI). In this model,
 we have implemented high-temperature heat integration across the
 reforming unit. The heat available in the syngas cooling train is

Table 1. Operating Conditions of the F–T Reactor

quantity	value
pressure	30 bar
temperature	520 K
per pass conversion	60%
α_{ASF} (eq 6)	0.97

Table 2. Steam Plant

pressure level	heat source
110 bar	high-temperature syngas cooling
48 bar	no heat source, steam production for reforming
18 bar	F–T reactor
5 bar	low-temperature syngas cooling

used to preheat the feeds to the reforming unit; excess heat is sent to the steam and power plant to produce electric power.

4. High-Temperature Heat Integration: Gas-Heated Reforming (GHR). From a process point of view, GHR requires more steam than ATR. In particular, to avoid the formation of coke, modern applications of GHR require a steam-to-carbon ratio (S/C) between 1.5 and 2.0. In this case, we have considered that this ratio can be lowered to 1.3.

5. Syngas Production via Ideal Catalytic Partial Oxidation (HTCPO and LTCPO). CPO is described by the following chemical reaction, eq 7:



Since reaction 7 is thermodynamically feasible at all temperatures ($\Delta G < 0$), we have set the reforming feed temperature in order to achieve the desired output temperatures (1300 and 700 K).

3.1. Motivation for Cases 1 and 2. F–T reactor performance depends on a wide list of parameters; however, we have considered only the effect of increasing catalyst selectivity (case 1) and per pass conversion of hydrogen (case 2). The rationale behind the choice of these parameters is the following: when catalyst selectivity is increased, there is a larger conversion of syngas into syncrude. However, the exergy F–T tailgas will be lower, and a larger amount of natural gas has to be provided to the fired heater to cover the heat demand of the process. This leads to two competing phenomena: a larger yield in the F–T unit and smaller syngas unit (increases efficiency) on one side and greater fuel consumption into the fired heater (reduces efficiency) on the other side. Although the process will always take advantage of increasing the F–T selectivity, a larger demand of natural gas in the fired heater will reduce the gain. We shall quantify these effects.

Enhanced per pass conversion of hydrogen may also play a role in the process efficiency. Due to the limited per pass conversion, F–T tailgases are recycled through the reactor to bring F–T unit hydrogen conversion to 90%. However, before recycling, tailgases are cooled to remove water. If per pass conversion of hydrogen can be increased to 90%, there is no need to recycle F–T tailgas, and heat losses due to thermal cycles are reduced. A quantification of this effect is provided.

3.2. Motivation for Cases 3–5. In cases 3–5, we show how to improve the performance of the syngas unit. Due to the large heat demand of the unit and to the large amount of heat made available in the syngas cooling train, a potential improvement is given by better heat management across the unit (cases 3 and 4).

Limitations to high-temperature heat integration (case 3) come from the high carbon activity of the syngas that promotes metal dusting¹⁸ on the metallic surfaces of the heat exchangers. Metal dusting is a corrosion process arising from the combined effect of carburization and oxidation that considerably shortens the lifetime of the tubes. The potential for metal dusting is very high in environments of fully converted syngas at high pressure and with a temperature range between 700 and 1100 K. To avoid metal dusting, hot syngas (1300 K) is quickly cooled in waste heat boilers where high-pressure steam is generated. The steel temperature in the waste heat boiler holds about the same temperature as the boiling

water, thereby minimizing metal dusting problems. To take into account the limitations that metal dusting puts on high-temperature heat integration, the flows upstream and downstream of the ATR do not exchange heat in our reference case. The *HTHI* case (case 3) was chosen to investigate the efficiency gain if corrosion due to metal dusting could be avoided, or, in other terms, how much exergy loss can be attributed to metal dusting.

Another way of integrating high-temperature heat across the reforming unit is via GHR (case 4). This was investigated in the *GHR* test case. GHR is a combination of autothermal and steam reforming. Heat for the endothermic steam reforming is provided by the hot ATR products. Details of the process can be found in Higman, van der Burgt²⁶ and Wesenberg.²⁷ In our case study, we have considered a GHR process with a steam reformer in series with an autothermal reformer. Natural gas is fed into a steam reformer that is heated by the hot ATR tailgas. After the steam reformer, partially converted syngas is mixed with oxygen and fully converted into the ATR. ATR products are cooled by exchanging heat in the steam reformer.

Test case 5 refers to an ideal CPO with no formation of CO_2 . The feasibility of this process has not been demonstrated yet, but since all of the carbon is converted into syngas with the desired H_2/CO ratio, we use it to set an upper limit for the syngas unit performance. However, the products are not stable, and there is a huge effort to develop catalysts able to avoid further oxidation of CO into CO_2 . The most promising technology to achieve CPO with a low level of formation of CO_2 is the so-called short contact time catalytic partial oxidation, see for example, Aartun, et. al.²⁹, Hickman, Schmidt³⁰ and Bizzi et. al.^{32,28–32} In these studies, the best catalyst performance is achieved at high temperatures (around 1000 K). We selected two temperatures for the products: a high temperature (1300 K) and a low one (700 K). The high-temperature case is meant to be compared with conventional ATR. The final products' temperature is the same, but while ATR suffers from selectivity losses (CO_2 production), HTCPO does not, so it was used to quantify the effect of selectivity losses on ATR. The product temperature for LTCPO was set to 700 K, to remain below the temperature limits set by metal dusting.

4. Calculation Procedures

Simulations were performed with the commercial package PRO/II version 7.1. The code computes, by means of an iterative method, thermodynamic properties of streams and process units in the steady state. In our model, we have chosen the Soave–Redlich–Kwong equation of state, and water properties were derived from steam tables. The code computes thermodynamic data of streams and operation units, and on the basis of these, we have performed the exergy analysis. PRO/II includes a tool for exergy computation, but due to a lack of references and to some uncertainties in the computation of chemical exergies, we have performed the exergy analysis using an electronic spreadsheet to compute physical and chemical exergy. Our computation is based on the method described by Szargut¹² and Kotas.¹⁹ The database for chemical exergies at a standard state was taken from Kotas.¹⁹

Results from the PRO/II simulations were analyzed at two levels: first, we checked mass and energy balances, and then we computed the exergy of the streams and the lost work of the units as the difference between input and output exergy. Mass balances were used primarily to check the computations' consistency, but

(27) Wesenberg, H. M. Gas Heated Steam Reformer Modelling. Ph.D. Thesis at NTNU (2006:77), Trondheim, Norway, 2006.

(28) Hansen, R. EFI Gas-to-Market Conference, Paris, France, Sept. 27–28, 2006.

(29) Aartun, I.; Venvik, H. J.; Holmen, A.; Pfeifer, P.; Görke, O.; Schubert, K. *Catal. Today* **2005**, *110* (1–2), 98–107.

(30) Hickman, D. A.; Schmidt, L. D. *J. Catal.* **1992**, *138* (1), 267–282.

(31) Rohde, M. P.; Unruh, D.; Schaub, G. *Catal. Today* **2005**, *106* (1–4), 143–148.

(32) Bizzi, M.; Basini, L.; Saracco, G.; Specchia, V. *Chem. Eng. J.* **2002**, *90* (1–2), 97–106.

Table 3. Inlet Composition

species	mass fraction
CO ₂	<1%
N ₂	4%
CH ₄	93%
C ₂ H ₆	2%
C ₃ H ₈	<1%
total flow rate	131 ton/h

they also give some interesting insights into the path that carbon follows from methane to synthetic hydrocarbon and into the mechanisms leading to CO₂ production. The input of natural gas to the process is kept constant for all cases calculated; its composition and flow rates are given in Table 3; the pressure is 75 bar and the temperature 320 K. The same modeling approach was followed in all the cases, ensuring consistency among the results.

The mass balances were used to follow the carbon path along the process. In particular, we are interested in studying how the carbon is used in the process, and how much of it is converted into products. This leads to two different formulations for the “use” of carbon in the ATR and the F–T unit. Since CO₂ does not take part in the Co-based F–T synthesis, we are interested in the CO yield of the syngas unit, as defined by eq 8 (CO yield):

$$Y_{CO} = \frac{m_{CO_{prod}}}{m_{CH_4,in} + m_{CO_2,in}} \quad (8)$$

The F–T unit consists of the F–T reactor itself plus the water separation and tailgas recycle loop (Figure 1). In our case, F–T products are modeled as a mixture of hydrocarbons with carbon numbers greater than 5 and smaller than 40, while the carbon source is the CO converted across the reactor. This leads to the following definition of the F–T reactor selectivity (eq 9):

$$S_{F-T} = \frac{\sum_{N=5}^{40} m_N N}{m_{CO_{reactor}}} \quad (9)$$

Since F–T tailgas is recycled to improve conversion, the F–T yield is defined as the ratio between the carbon products and the CO converted across the whole F–T unit.

$$Y_{F-T} = \frac{\sum_{N=5}^{40} m_N \cdot N}{m_{CO_{unit}}} \quad (10)$$

In the reference case analysis, we fixed the F–T unit yield to be 90%. The rationale behind this choice is that, since CO₂ does not react in the F–T reactor, it builds up in the F–T loop, increasing the mass flow up to a level where both the pipes and the reactor itself become too large. In our case, the 90% limit ensures that the diameter of the reactor is less than or equal to 12 m.

The exergetic efficiency was computed using eq 11

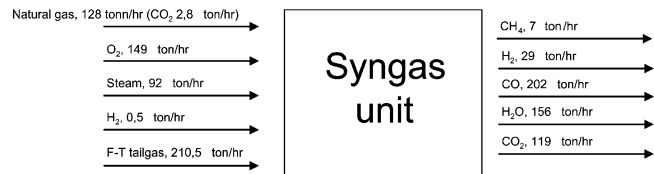
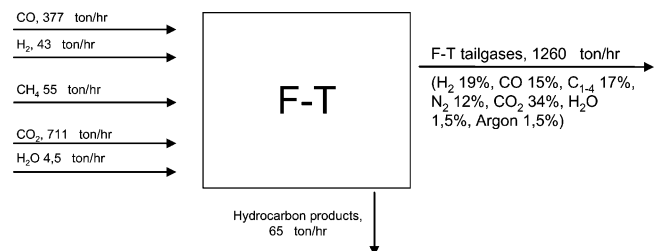
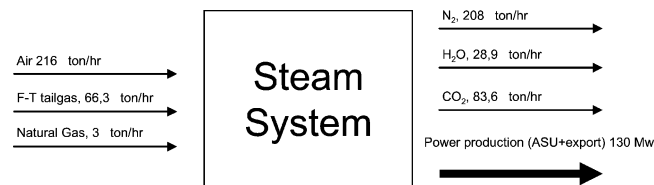
$$\eta_{ex} = \frac{E_{wax} + P_{el}}{E_{NatGas}} \quad (11)$$

where E_{wax} is the exergy of the hydrocarbon wax, P_{el} is the surplus electric power produced from recovered steam, and E_{NatGas} is the exergy of the natural gas (47.3 MJ/kg). Units’ irreversibilities were computed on the basis of the difference between input and output exergy. Two different flow sheets were used, one for the GTL process and one for the steam plant. The two processes exchange both work (mechanical and electric power) and heat.

384

5. Results

5.1. Reference Case. The first conversion in the GTL process occurs in the syngas unit, where natural gas is mixed with F–T


Figure 2. Process mass balance.

Figure 3. Syngas unit mass balance.

Figure 4. F–T reactor mass balance.

Figure 5. Steam system mass balance.

unit tailgas and converted into syngas. The CO yield resulting from the chemical equilibrium in the ATR (eq 8) is $Y_{CO} = 70\%$.

The results of the mass balance calculations are shown in Figures 2–5. Figure 2 gives the overall mass balance for the main species involved in the process.

The ATR mass balance is shown in Figure 3. The conversion of natural gas is almost complete (>95%), and on a mass basis, the production of CO₂ is relatively low. The F–T reactor mass balance shows (Figure 4) that CO (the feed gas with H₂) conversion is not complete. In particular, CO conversion is about 50%, while H₂ conversion was fixed at 60%. The F–T mass balance also shows that a large amount of water is produced in the reactor. Figure 5 gives the steam system mass balance.

5.2. Exergy Analysis, Reference Case. The results of the exergy computations are summarized in a Grassman diagram in Figure 6. The exergy efficiency of the reference case was $\eta_{ex} = 62\%$; the production of power accounts for 5% of the overall process output.

The Grassman diagram clearly shows how the F–T tailgas loop recycles a large amount of exergy. The main source of irreversibilities is the syngas production unit (60%). The power plant, ASU, and F–T account for the remaining 40% of the losses as reported in Figure 7.

5.2.1. Performance of the Syngas Production Unit. We present the lost work in two different manners: Figure 7 shows the lost work for each unit, while Table 4 reports the lost work of the reforming unit including preheating, reforming, and ASU. Although the ASU is powered by the power plant, it is allocated to the reforming unit because oxygen production is required only by the reforming process.

 385
386

 387
388
389
390
391
392
393
394
395
396
397
398
399
400
401
402
403
404
405
406
407
408
409
410
411
412
413
414
415
416

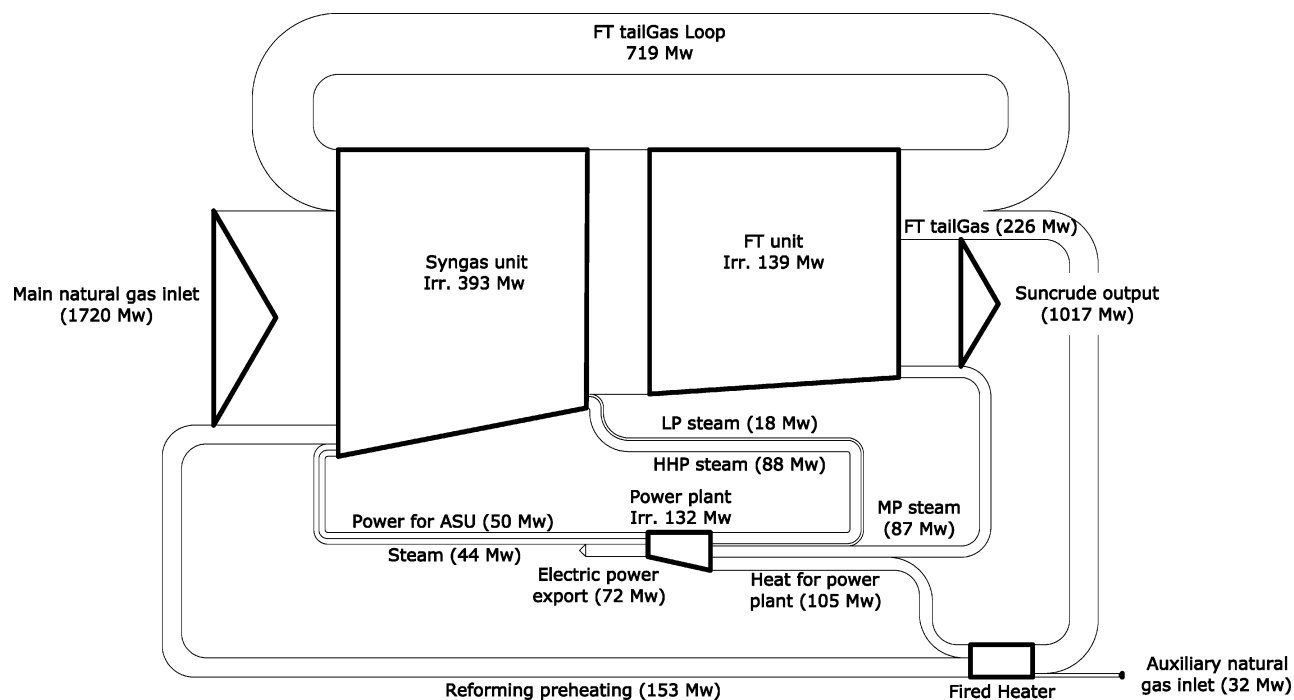


Figure 6. Grassman diagram of the GTL process. Streams with exergy below 15 MW are not shown. Fired heater losses are allocated to the power plant and the syngas unit.

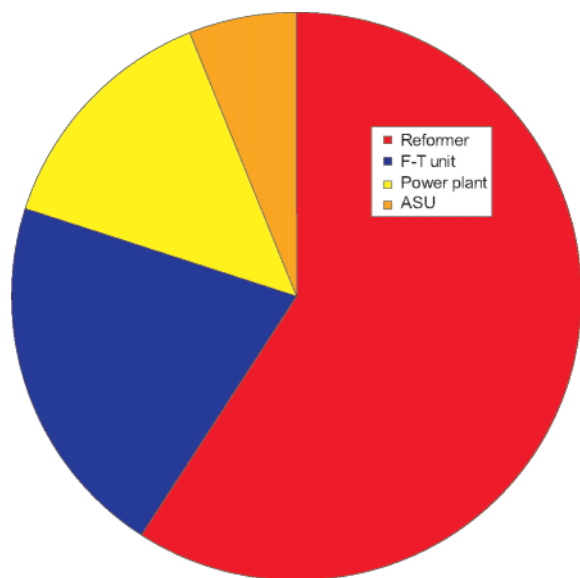


Figure 7. Main irreversibilities sources.

Table 4. Syngas Unit Plus ASU Lost Work

unit	lost work
preheating	7%
reactor	33%
cooling	20%
ASU	9%
total	69%

5.3. Performance of the F–T Unit. In contrast with the ATR, the F–T reactor is not adiabatic, and heat must be recovered directly from it to keep the operating temperature constant. This helps to reach a high exergetic efficiency of 93%.

5.4. The Steam System. The power plant uses surplus heat recovered from the F–T unit and syngas unit to generate power from steam. Since heat recovery from the syngas unit as well as heat recovery from the F–T reactor cannot produce superheated steam, the heat needed for steam superheating is provided from burning the F–T tailgas and natural gas. The efficiency

Table 5. Steam System Lost Work

unit	lost work
power production	6%
steam production	5%
total	11%

of the power plant is about 30%. A more efficient cogeneration process could be coupled to the GTL plant to improve the efficiency of power production. In Table 5, we have reported lost work in the steam system to produce the power for both ASU and electricity.

5.5. Test Cases. In order to compare the test cases, we show the variation in lost work of the three macro units: power plant, syngas production unit with ASU, and F–T unit. A synopsis of the results showing the result of the exergy analysis in all cases is reported in Figure 8. The analysis shows that the lost work in the GTL process can be reduced both by improving the process selectivity and by implementing GHR.

Once-through operation of the F–T reactor has very little effect on the lost work.

In Figure 9, we show how the efficiency is affected by F–T selectivity. According to the figure, as selectivity increases by 5%, the efficiency increases by 3%.

The GHR reduces lost work by 2%. F–T reactor lost work is not affected by it, while the reforming step itself is more efficient. Because the need of steam in the reforming unit with GHR is twice that of ATR, the power plant shows a slight increase in the lost work.

High-temperature heat integration has a large potential to improve the GTL efficiency. Clearly, the gain is achieved in the reforming unit; the losses due to gas preheating (lumped in the reforming unit losses) are reduced by 6% compared to the reference case. However, due to the increased losses in the power plant, the overall efficiency is not largely affected.

It is not surprising that ideal catalytic partial oxidation (no CO₂ production) leads to the best results, since reforming is the most dissipative step in GTL. In low-temperature CPO, the lost work is less than 30%, and all the gain is achieved in the

417
418
419
420
421
422
423
424
425
426

427
428
429
430
431
432
433
434
435
436
437
438
439
440
441
442
443
444
445
446
447
448
449
450
451
452
453
454
455
456
457
458

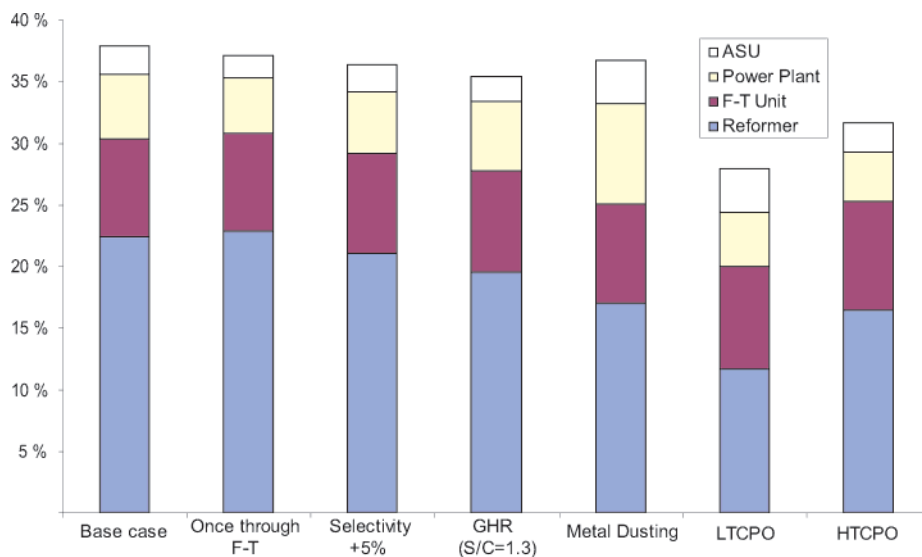


Figure 8. Lost work.

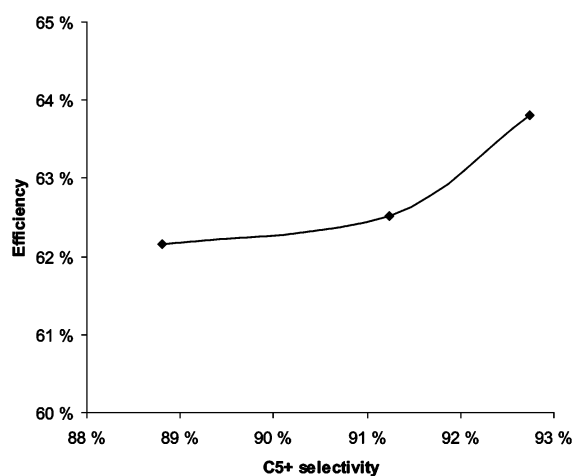


Figure 9. Effect of F-T selectivity on the process efficiency.

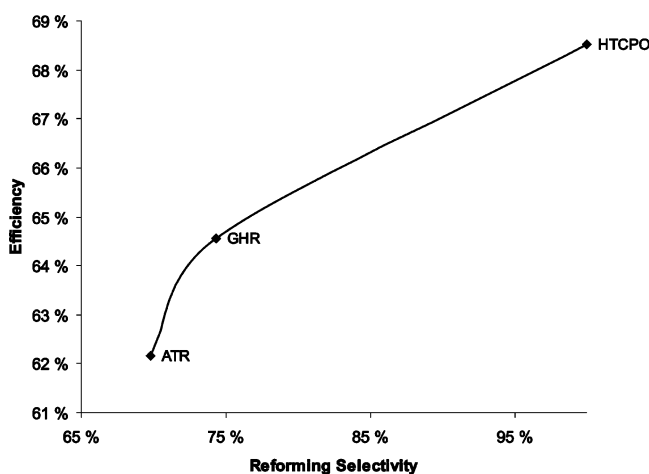
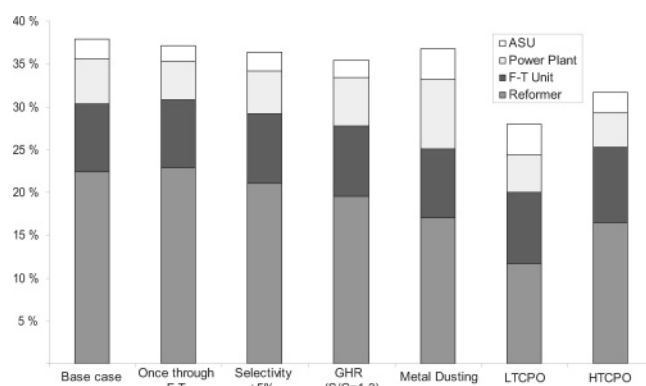


Figure 10. Process efficiency as a function of reforming selectivity.

459 reforming unit. High-temperature CPO was instead investigated
 460 to show the impact of selectivity losses on the process efficiency
 461 compared with ATR. In Figure 10, we report the GTL efficiency
 462 as a function of the CO yield in the reforming defined by eq 8.
 463 The three cases correspond to three different technologies: ATR,
 464 GHR, and HTCPO. For ATR, the CO yield is 70%; for GHR,
 465 it is 74%, and for HTCPO, it is 100% (no CO₂ formation from
 466 reforming). We used these three cases to assess how selectivity

Figure 11. Normalized CO₂ production.

467 losses in the reforming affect GTL efficiency. HTCPO, ATR, and
 468 GHR produce syngas at similar temperatures; therefore, losses
 469 due to preheating and cooling of the syngas are similar. Moreover,
 470 Figure 8 shows that losses in the F-T unit are almost identical,
 471 while there are only minor differences in the power unit lost work,
 472 mostly due to the different needs of steam. Figure 10 shows that,
 473 compared to the reference case, selectivity losses in the reforming
 474 unit account for 6% of the overall losses.

475 **5.6. Carbon Conversion and CO₂ Emissions.** In order to
 476 report CO₂ production, we computed the ratio between the number
 477 of moles of CO₂ produced by the process and the number of moles
 478 of carbon in the natural gas feeds (both GTL and fired heater).
 479

480 Figure 11 shows that about 24% of the carbon is converted into
 481 CO₂ in the reference case. This value can be reduced by 3–4%
 482 implemented either by GHR or by improved F-T selectivity (better
 483 catalyst).

484 6. Discussion

485 The major exergy consumer in a GTL process is the reforming
 486 unit, which accounts for 69% of the overall losses when ASU
 487 losses are included. Our exergy analysis shows that losses are
 488 mostly due to the chemical conversion process (33%). In particular,
 489 it is possible to identify two kinds of losses: one that occurs also
 490 in the ideal process and another due to CO₂ production (low
 491 selectivity). Ideal catalytic partial oxidation as described by eq 7
 492 converts the whole natural gas into a syngas whose composition is
 493 perfectly suited for F-T synthesis. By

494 computing the change in exergy of reagents (CH₄ and O₂) and
 495 products (CO and H₂), it turns out that 11% of the exergy is
 496 lost. This loss cannot be minimized and should be considered
 497 as unavoidable. The second kind of chemical loss is due to CO₂
 498 production in the reforming unit and was outlined comparing
 499 ATR, GHR, and HTCPO. In the reference case, selectivity losses
 500 in the ATR accounted for about 6% of the overall losses of the
 501 plant and may be reduced if the CO yield could be increased.

502 Gas preheating occurs in a fired heater; losses are due to heat
 503 exchange and can be reduced if reforming takes place at lower
 504 temperatures or via HTHI or a more tailored temperature
 505 profile.²³ Syngas cooling is also highly dissipative, and although
 506 a large amount of heat is recovered in the power plant, entropy
 507 production is large. High-temperature heat integration can help
 508 to reduce these losses, allowing the use of about 30% of the
 509 latent heat to preheat the reforming unit feeds. However, a large
 510 amount of heat is made available in the fired heater and could
 511 be used to maximize the efficiency of the process. In our model,
 512 we kept the process layout constant; therefore, a larger amount
 513 of heat was used in a power plant with low efficiency, as also
 514 observed by Prins et al.³ for their BTL process. This explains
 515 why the exergetic efficiency of the process is not larger while
 516 HTHI reduces reforming losses by 6%. The fact that syngas
 517 production must take place at around 1300 K (ATR) is a major
 518 source of exergy loss in all GTL plants.

519 The ASU is also an important exergy consumer. In the
 520 reference case, its operation accounts for 9% of the lost work.

521 The F–T unit based on a LTFT slurry-phase cobalt catalyst
 522 is very efficient from an exergetic point of view, as was also
 523 observed by others.³ Reduced hydrogen conversion has a minor
 524 effect on the process; a slight gain is due to the fact that the
 525 mass flow of the F–T reactor tailgas recycled in the reforming
 526 unit is about 30% lower. This means that less heat has to be
 527 used to preheat the feed to the reforming unit, and more heat
 528 can be used in the power plant to produce steam and power.

529 Improving catalyst selectivity by 5% can effectively improve
 530 the GTL performance. It leads to two competing phenomena:
 531 on one side, the higher the selectivity, the larger the yield; on
 532 the other side, the higher the selectivity, the lower the exergy
 533 of the tailgas burned in the fired heater. The result is that the
 534 external supply of natural gas to the fired heater has to be
 535 increased. The unit that benefits the most from the increased
 536 selectivity is the reforming unit: when the yield is increased in
 537 the F–T unit, less light hydrocarbons have to be reconverted
 538 in the reforming unit. This reduces the size of the unit, the
 539 oxygen demand (ASU can be smaller), and the heat losses. The
 540 lost work in the power unit is also reduced, while the lost work
 541 in the F–T unit increases slightly due to the larger heat release.

542 In GTL processes, CO₂ production occurs both in the
 543 reforming unit and in the fired heater. In the results reported in
 544 Figure 11, we did not take any credit for the production of
 545 electric power (also referred to as “electric credit”). An analysis
 546 showing the carbon efficiency with electric credit was presented
 547 by Hansen²⁸ and shows that both GHR and catalyst selectivity
 548 improvements can reduce CO₂ emissions down to a level that
 549 would make GTL carbon efficiency similar to that of conven-
 550 tional oil refinery routes.

551 **7. Conclusion and Outlook**

552 In this study, we have analyzed the carbon path and exergy
 553 efficiency of a GTL process based on promising available
 554 technologies: syngas production by autothermal reforming and
 555 F–T technology based on a low-temperature slurry-phase
 556 reactor with a cobalt catalyst. Our aim was to set up a solid

reference case meant to show the performance of the whole 557
 process and the lost work (entropy production) in each unit. 558
 The analysis has shown that the reforming unit is the main 559
 exergy consumer (69%, ASU losses allocated to the reforming 560
 unit), followed by the F–T unit and power production (both 561
 about 20%), and that the GTL efficiency is on the order of 62%. 562

563 On the basis of a simulation model for the integrated syngas
 564 and F–T units, the effect of changing some key process
 565 parameters was studied. In the F–T unit, we looked at catalyst
 566 selectivity and per pass conversion. While increasing per pass
 567 conversion up to 90% does not affect the process efficiency,
 568 improving catalyst selectivity by 5% increases efficiency by
 569 2–3%.

570 In the syngas unit, we studied the effect of introducing high-
 571 temperature heat integration and increasing CO selectivity. A
 572 first case showed that high-temperature heat integration would
 573 make more heat available for the production of power, leading
 574 to an increase of the process performance by 1.5%. A better
 575 performance is achievable implementing GHR, which is also a
 576 way of integrating high-temperature heat. In addition, it also
 577 improves the reforming selectivity by 4% compared to that of
 578 ATR. If GHR with a steam-to-carbon ratio of 1.3 is achievable,
 579 the efficiency of GTL would increase by 2.5%.

580 An ideal LTCPO model was also tested. Although LTCPO
 581 has not been demonstrated as being feasible yet, it sets an upper
 582 limit for reforming technology applied for GTL. The efficiency
 583 for the GTL process with LTCPO is 70%. Finally, a HTCPO
 584 reformer was modeled to establish a trend between GTL
 585 performance and selectivity losses in the reforming unit.

586 CO₂ emissions were also investigated. In the reference case,
 587 about 24% of the carbon is converted into CO₂, and this is due
 588 both to selectivity losses in the reforming unit and to the carbon
 589 burned in the fired heater. By operating the GHR at a steam-
 590 to-carbon ratio of 1.3 or increasing F–T selectivity by 5%, the
 591 carbon efficiency in a GTL plant will improve by 3–4%.

592 **Nomenclature**

- 593 ATR = autothermal reformer
- 594 BTL = biomass-to-liquid
- 595 CTL = coal-to-liquid
- 596 CPO = catalytic partial oxidation
- 597 CSTR = continuously stirred tank reactor
- 598 GTL = gas-to-liquid
- 599 F–T = Fischer–Tropsch
- 600 GHR = gas-heated reforming
- 601 HTCPO = high-temperature catalytic partial oxidation
- 602 LTCPO = low-temperature catalytic partial oxidation
- 603 s/c ratio = steam-to-carbon ratio

604 **Acknowledgment.** We thank the Vista project of STATOIL
 605 and the Norwegian Academy for Science and Letters for financial
 606 support and Roger Hansen from STATOIL for substantial help in
 607 the definition of the problem and for technical support throughout
 608 the project.
 609 EF060646Y